CRYSTALLOGRAPHIC COMMUNICATIONS

ISSN 2056-9890

Refinement of $K[HgI_3]\cdot H_2O$ using non-spherical atomic form factors

Misael Chocolatl Torres, Sylvain Bernès* and Ulises Salazar Kuri

Instituto de Física, Benemérita Universidad Autónoma de Puebla, 72570 Puebla, Pue., Mexico. *Correspondence e-mail: sylvain_bernes@hotmail.com

Received 10 May 2021
Accepted 31 May 2021

Edited by M. Weil, Vienna University of Technology, Austria

Keywords: crystal structure; redetermination; atomic form factors; NoSpherA2.

CCDC reference: 2087087

Supporting information: this article has supporting information at journals.iucr.org/e

The crystal structure model for potassium triiodidomercurate(II) monohydrate, $K[HgI_3]\cdot H_2O$, based on single-crystal data, was reported 50 years ago [Nyqvist & Johansson (1971). *Acta Chem. Scand*. **25**, 1615–1629]. We have now redetermined this structure with X-ray diffraction data at 0.70 Å resolution collected at 153 K using Ag *Kα* radiation. Combined quantum mechanical methods (*ORCA*) and computation of non-spherical scattering form factors (*NoSpherA2*) allowed the refinement of the shape of the water molecule with anisotropic H atoms, despite the presence of heavy elements in the crystal. The refined shape of the water molecule *via* this Hirshfeld refinement is close to that determined for liquid water by neutron diffraction experiments. Moreover, the Laplacian of the electron density clearly shows how electron density accumulates along the O—H *σ*-valence bonds in the water molecule.

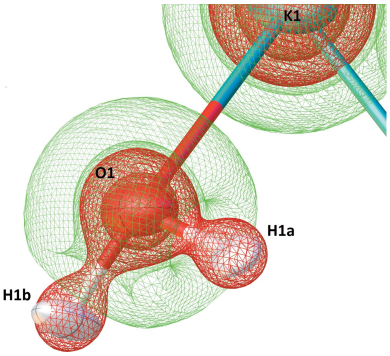

1. Chemical context

It is well known that the 'independent atom model' (IAM), universally implemented in mainstream X-ray crystallography software, has the drawback of affording insufficient crystal structure models. Given that a spherical distribution of electron density around each atom is assumed, for example, by using the Cromer–Mann parameterization of the non-dispersive part of the form factors, any density involved in bonds, lone pairs and intermolecular charge transfer is completely ignored. In this context, satisfactory structure models can be obtained only on the basis of neutron diffraction data. An extreme case of discrepancy between results obtained with both radiations is the O—H bond length for the hydroxyl group in alcohols and water, which is underestimated by *ca* 20% by X-rays. However, neutron diffraction facilities are scarce, and even non-existent in underdeveloped countries. As a matter of fact, only 0.2% of the structures currently deposited in the CSD originate from neutron diffraction studies (Groom *et al.*, 2016).

Within many approaches available to overcome this issue, the 'Hirshfeld atom refinement' (HAR; Capelli *et al.*, 2014) strategy is gaining popularity. After calculating a molecular wave function for a structural model (not necessarily limited to the asymmetric unit), the electronic density functions of the so-called Hirshfeld atoms are extracted through a partitioning process (Hirshfeld, 1977), and eventually Fourier transformed, to afford non-spherical scattering factors for each individual atom in the real space and each reflection in the reciprocal space. More accurate structure factors can then be calculated during a least-squares refinement, and the full process can be iterated until convergence.

A user-friendly implementation of HAR has been recently released with *OLEX2* (version 1.3) and is fully interfaced with the *olex2.refine* least-squares engine (Kleemiss *et al.*, 2021). This new tool, coined as *NoSpherA2* (pronounced 'Nosferatu'), is virtually universal since any element can be present in the structure. Moreover, the structure can be disordered, with atoms in special positions, squeezed with a solvent mask, or can include restrained parts. Twinned crystals can also be handled in the same way as single crystals, by computing a single wave function for each twin component. Finally, data resolution is not a concern, as long as atomic resolution is achieved [$d_{\min}$ = 0.84 Å, corresponding to $(\sin\theta/\lambda)_{\max} = 0.6$ Å^{-1}]. At worst, a data set with no information at all about aspherical local densities would give a Hirshfeld refinement close to that obtained with Cromer–Mann form factors.

So far, HAR has been used mainly for organic compounds, for at least two reasons. Many accurate orbital basis sets are available for light elements and, more significantly, this class of molecules is the most interesting one for such refinements: organic compounds include a large variety of chemical bonds (σ, π, aromatic, 2*c*–3*e* bonds, *etc.*) and heteroatoms frequently bear electron lone pairs. The structural model obtained *via* HAR is thus expected to be greatly improved compared to that derived from a traditional refinement with spherical densities.

We used *NoSpherA2* to refine the crystal structure of a material including both heavy and light elements, with the aim of assessing whether a non-spherical refinement is suitable and useful for such materials. The matter has been already studied for challenging compounds, namely transition-metal hydrides (Woińska *et al.*, 2021; Kleemiss *et al.*, 2021), and is now extended to an iodidomercurate hydrate, K[HgI$_3$]·H$_2$O.

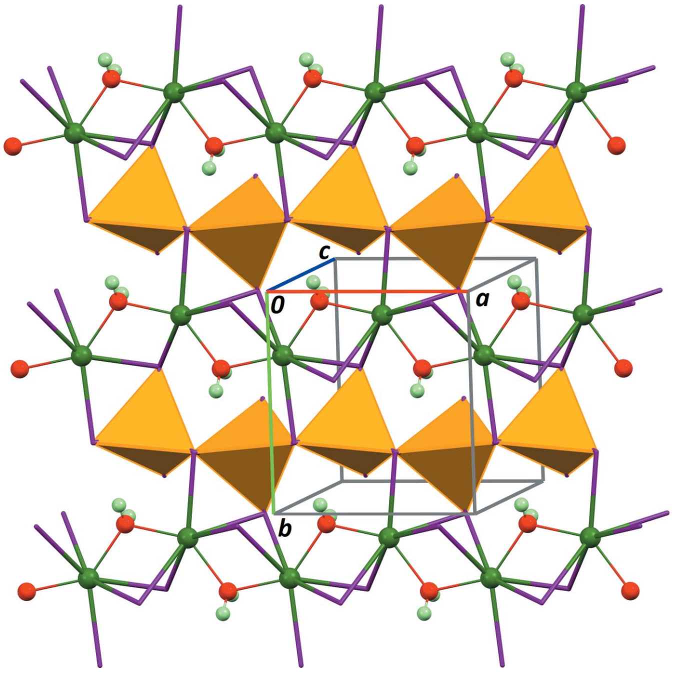

Figure 1
Part of the crystal structure of the title compound. Colour code: orange = [HgI$_4$] tetrahedra, purple = I, green = K, red = O, pale green = H.

Table 1
Experimental details.

Crystal data	
Chemical formula	K[HgI$_3$]·H$_2$O
M_r	638.41
Crystal system, space group	Orthorhombic, *Pna*2$_1$
Temperature (K)	153
a, *b*, *c* (Å)	8.5810 (2), 9.2648 (3), 11.4073 (4)
V (Å^3)	906.89 (5)
Z	4
Radiation type	Ag *Kα*, λ = 0.56083 Å
μ (mm^{-1})	14.87
Crystal size (mm)	0.06 × 0.05 × 0.03
Data collection	
Diffractometer	Stoe Stadivari
Absorption correction	Multi-scan (*X-AREA*; Stoe & Cie, 2019)
$T_{\min}$, $T_{\max}$	0.064, 0.132
No. of measured, independent and observed [$I > 2\sigma(I)$] reflections	29699, 2720, 2179
$R_{\rm int}$	0.070
$(\sin\theta/\lambda)_{\max}$ (Å^{-1})	0.714
Refinement	
$R[F^2 > 2\sigma(F^2)]$, $wR(F^2)$, S	0.021, 0.038, 0.87
No. of reflections	2720
No. of parameters	74
No. of restraints	21
H-atom treatment	All H-atom parameters refined
$\Delta\rho_{\max}$, $\Delta\rho_{\min}$ (e Å^{-3})	1.17, −1.26
Absolute structure	Flack (1983)
Absolute structure parameter	0.033 (11)

Computer programs: *X-AREA* (Stoe & Cie, 2019), *SHELXT2018/2* (Sheldrick, 2015*a*), *olex2.refine 1.3* (Bourhis *et al.*, 2015), *OLEX2* (Dolomanov *et al.*, 2009), *Mercury* (Macrae *et al.*, 2020) and *publCIF* (Westrip, 2010).

2. Structural commentary

The crystal structure of potassium triiodidomercurate(II) monohydrate, K[HgI$_3$]·H$_2$O, was reported 50 years ago, using data collected on a Philips–Norelco PAILRED diffractometer, with monochromatized Mo *K* radiation (1542 reflections in the 0*kl*–10*kl* half-sphere; *R* = 0.081 for an anisotropic model omitting H atoms; Nyqvist & Johansson, 1971). The powder diffraction pattern is also deposited in the PDF-2 database, with reference PDF 00-027-0415 (Gates-Rector & Blanton, 2019). Using low-temperature data collected with Ag *Kα* radiation, we now obtained the same structure at 0.70 Å resolution in the same space group, *Pna*2$_1$ (Fig. 1 and Table 1). The Hg atoms form distorted [HgI$_4$] tetrahedra sharing one corner and giving a chain structure along the *a*-axis direction. Water molecules bridge K$^+$ cations and are sandwiched between these chains, at normal distances, K—OH$_2$ $\simeq$ 2.75 Å. The cations are seven-coordinate, a common coordination number for K$^+$, characterized by its large ionic radius. The three-dimensional structure is completed by K$^+$ cations bridging [HgI$_4$] tetrahedra in neighbouring chains. The water molecules are oriented in such a way that O—H···I hydrogen bonds are formed with two I atoms on the edge of an [HgI$_4$] tetrahedron.

Although H atoms were visible in a difference-Fourier map, the IAM refinement carried out with *SHELXL* (Sheldrick, 2015*b*) gave an odd shape for the water molecule. Hydroxyl O—H groups were then restrained to have the same bond lengths with an effective standard deviation of 0.04 Å. Rigid bond restraints with a standard deviation of 0.008 Å for 1,2 and 1,3 distances in the K/O1/H1*a*/H1*b* fragment were also applied. Both O—H bond lengths in the water molecule converged to 0.84 (11) Å, and the H—O—H angle was too acute, 87 (10)°. Moreover, isotropic displacement parameters for the H1*a* and H1*b* atoms were unbalanced, 0.06 (5) and 0.18 (9) Å^2, respectively. For this preliminary refinement, hydrogen bonds were determined with large uncertainties for O—H···I angles, 160 (12) and 159 (26)°.

With the hope of improving the shape of the water molecule, a non-spherical refinement was carried out using the *SHELXL* model as a starting point. The wave functions were calculated using *ORCA* with the two-component relativistic basis set x2c-TZVPP and the generalized gradient approximation PBE functional (Neese, 2018). The least-squares refinements were then carried out with *olex2.refine* (Bourhis *et al.*, 2015), while keeping the same restraints as for the *SHELXL* refinement. For the final calculation of non-spherical form factors with *NoSpherA2*, a neutral dimeric cluster [KHgI$_3$·H$_2$O]$_2$ was used as a structure model, in order to take into account O—H···I hydrogen bonds. The final refinement was done with *olex2.refine* (Table 1), and a comparison of the asymmetric units for the IAM and HAR refinements is given in Fig. 2.

The heavy part of the structure is almost unchanged after HAR, as expected. When comparing bonds lengths and angles, the largest difference is observed for the K—O bonds, with a shift of 0.006 Å; for bond angles, the largest difference between the two refinements is 0.25° for the angle K1—O1—K1^{i} [symmetry code: (i) $x + \frac{1}{2}, -y + \frac{1}{2}, z$]. Moreover, uncertainties for bond lengths and angles are systematically improved with HAR. Likewise, displacement parameters for Hg, I and K atoms are almost unaffected after using non-spherical form factors. In contrast, the water molecule clearly displays a more accurate shape. Bond lengths for the O—H groups are 1.07 (6) and 1.11 (7) Å for the HAR model, with an H—O—H angle of 107 (8)°. For liquid water, neutron diffraction experiments afforded O—H = 0.970 ± 0.005 Å and H—O—H = 106.1 ± 1.8° (Ichikawa *et al.*, 1991; Milovanović *et al.*, 2020). These dimensions are also consistent with the shape previously described for a water molecule bridging two K$^+$ cations in a potassium aryloxide aggregate characterized by neutron diffraction at 100 K: O—H = 0.963 (16)–1.009 (16) Å and H—O—H = 108.0 (13)° (Morris *et al.*, 2007). It was possible to refine anisotropic displacement parameters for the H atoms, although it was necessary to use rigid bond restraints for the K—OH$_2$ group, in order to avoid non-positive definite H atoms. In the final model, displacement ellipsoids for H atoms are well balanced (Fig. 2).

The final residual map is featureless, but the deformation density map in the water molecule vicinity is insightful (Fig. 3). A positive density close to the O atom reflects the presence of electron lone pairs, while a negative density centred on the H-atom sites indicates the positively charged character of the H atoms, as a consequence of the difference of electronegativity with the O atom. A diffuse positive density is even visible at the midpoint of the O—H bonds, related to the contribution of the covalent σ-bonds to non-spherical densities. Beyond features observed for the water molecule, the deformation map is flat, confirming that a Hirshfeld refinement adds very

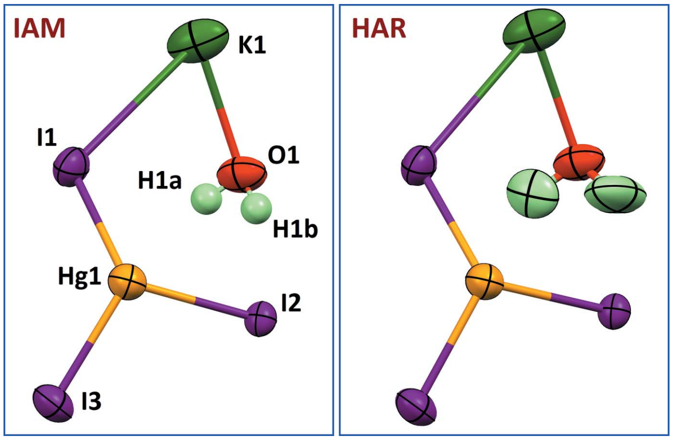

Figure 2
Ellipsoid plots of the asymmetric unit for the IAM (left) and HAR (right) models, with displacement ellipsoids at the 85% probability level. For the IAM refinement, isotropic H atoms are shown as spheres of arbitrary radius, while anisotropic H atoms in the HAR panel are shown with their refined ADPs.

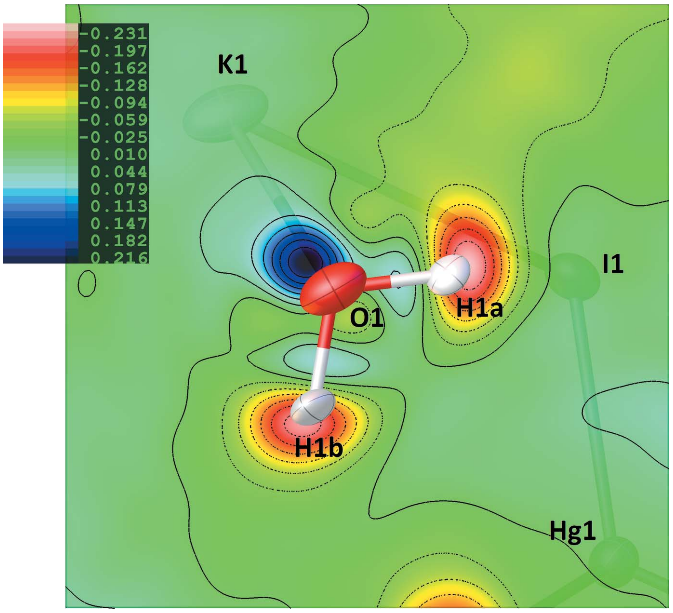

Figure 3
HAR – IAM dynamic deformation density map in the plane of the water molecule. Isolevel contours for positive density (e$^-$/A^3) are displayed as solid lines with the map coloured blue, while isolevel contours for negative density are displayed as dashed lines, with the map coloured red. The map was plotted with *OLEX2* (Dolomanov *et al.*, 2009).

Acta Cryst. (2021). E**77**, 681–685 Chocolatl Torres *et al.* • K[HgI$_3$]·H$_2$O **683**

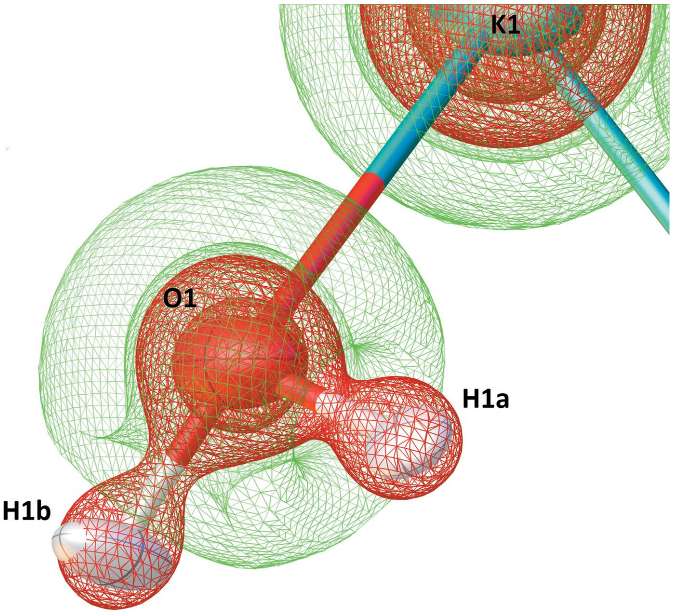

Figure 4
Three-dimensional wire map of the Laplacian of the electron density in the vicinity of the water molecule, at ±0.25 $e^{-}/Å^{5}$ level. The positive isosurfaces (green) show where electron density depletion occurs (valence-atomic orbital regions), while negative isosurfaces (red) show regions where electron density accumulates (bonding-electrons energy densities). The map was calculated on a 0.05 Å grid in real space and was generated with *OLEX2* (Dolomanov *et al.*, 2009).

little to the conventional IAM approximation in those parts. Finally, the Laplacian of the electron density, $\nabla^2\rho$, also shows expected features. Electronic density is locally concentrated over the attractive covalent O—H σ-bonds in the water molecule (Fig. 4), while heavy atoms display $\nabla^2\rho(x, y, z)$ isosurfaces with spherical symmetry.

3. Discussion and conclusions

Regarding the crystal structure refinement, the drop for residuals R_1 and wR_2 is marginal with a HAR compared to a IAM refinement with *SHELXL*, at any resolution, since the structure-factor amplitudes are dominated by the contribution of heavy scatterers, Hg and I. However, in the present case, diffraction data contain information about the non-sphericity of the form factors for the O and H atoms, warranting a HAR. Given that computational cost associated with the calculation of the wave function increases drastically for large molecular systems or large clusters of molecules, HAR may prove challenging to implement as a day-to-day routine, as long as desktop computers are used for structure refinements. However, the refinement reported here shows that an alternative would be to perform refinements through a hybrid IAM/HAR strategy, with structure factors including conventional spherical form factors for heavy atoms, and non-spherical form factors for light atoms. Obviously, this may not apply to large organic systems, like proteins, unless super-computing is involved (Capelli *et al.*, 2014).

4. Synthesis and crystallization

Caution!! Any mercury compound poses potential health risks; appropriate safety precautions and disposal procedures must be taken to handle the complexes here reported.

The compound under study was obtained as a by-product during the synthesis of $Ag_2[HgI_4]$. A procedure to obtain $Ag_2[HgI_4]$ single crystals involves the near saturation of $K_2[HgI_4]$ with HgI_2 and AgI in an aqueous medium (Browall *et al.*, 1974). Potassium tetraiodomercurate(II), commonly known as Nessler reagent, was obtained by dissolving 2.603 g of KI and 3.574 g of HgI_2 in an aqueous medium, following the reaction: $HgI_2 + 2\ KI \rightarrow K_2[HgI_4]$. The resulting solution was nearly saturated with HgI_2 and subsequently with AgI. The solution was kept under constant stirring for 30 min at 323 K. After that, the solution was stored in 50 ml plastic tubes in complete darkness for one month.

The crystals obtained were washed with a 2 *M* solution of $K_2[HgI_4]$ and distilled water. Since the process for the preparation of these compounds contains the precursors HgI_2 and KI in an aqueous medium, this also favours the crystallization of $K[HgI_3]\cdot H_2O$ within a temperature range of 273–353 K (Sieskind *et al.*, 1998). One small crystal of $K[HgI_3]\cdot H_2O$ recovered from such a crystallization was used for the present study.

5. Refinement details

Crystal data, data collection, and structure refinement details for the last least-squares cycle of *olex2.refine* are summarized in Table 1. All atoms were refined anisotropically. In the water molecule, O—H bonds were restrained to have the same length, with a standard deviation of 0.04 Å. Rigid bond restraints with a standard deviation of 0.008 Å for 1,2 and 1,3 distances in the K—OH_2 fragment were also applied.

Acknowledgements

We are grateful to Dr Florian Kleemiss (Olexsys Ltd, UK) for helpful guidance during the refinement of the structure and for the continuous development of *NoSpherA2*.

Funding information

Funding for this research was provided by: Consejo Nacional de Ciencia y Tecnología (grant No. 268178; grant No. A1-S-10011).

References

Bourhis, L. J., Dolomanov, O. V., Gildea, R. J., Howard, J. A. K. & Puschmann, H. (2015). *Acta Cryst.* A**71**, 59–75.
Browall, K. W., Kasper, J. S. & Wiedemeier, H. (1974). *J. Solid State Chem.* **10**, 20–28.
Capelli, S. C., Bürgi, H.-B., Dittrich, B., Grabowsky, S. & Jayatilaka, D. (2014). *IUCrJ*, **1**, 361–379.
Dolomanov, O. V., Bourhis, L. J., Gildea, R. J., Howard, J. A. K. & Puschmann, H. (2009). *J. Appl. Cryst.* **42**, 339–341.
Flack, H. D. (1983). *Acta Cryst.* A**39**, 876–881.
Gates-Rector, S. & Blanton, T. (2019). *Powder Diffr.* **34**, 352–360.

Groom, C. R., Bruno, I. J., Lightfoot, M. P. & Ward, S. C. (2016). *Acta Cryst.* B**72**, 171–179.

Hirshfeld, F. L. (1977). *Theor. Chim. Acta*, **44**, 129–138.

Ichikawa, K., Kameda, Y., Yamaguchi, T., Wakita, H. & Misawa, M. (1991). *Mol. Phys.* **73**, 79–86.

Kleemiss, F., Dolomanov, O. V., Bodensteiner, M., Peyerimhoff, N., Midgley, L., Bourhis, L. J., Genoni, A., Malaspina, L. A., Jayatilaka, D., Spencer, J. L., White, F., Grundkötter-Stock, B., Steinhauer, S., Lentz, D., Puschmann, H. & Grabowsky, S. (2021). *Chem. Sci.* **12**, 1675–1692.

Macrae, C. F., Sovago, I., Cottrell, S. J., Galek, P. T. A., McCabe, P., Pidcock, E., Platings, M., Shields, G. P., Stevens, J. S., Towler, M. & Wood, P. A. (2020). *J. Appl. Cryst.* **53**, 226–235.

Milovanović, M. R., Živković, J. M., Ninković, D. B., Stanković, I. M. & Zarić, S. D. (2020). *Phys. Chem. Chem. Phys.* **22**, 4138–4143.

Morris, J. J., Noll, B. C., Schultz, A. J., Piccoli, P. M. B. & Henderson, K. W. (2007). *Inorg. Chem.* **46**, 10473–10475.

Neese, F. (2018). *WIREs Comput. Mol. Sci.* **8**, e1327.

Nyqvist, L. & Johansson, G. (1971). *Acta Chem. Scand.* **25**, 1615–1629.

Sheldrick, G. M. (2015*a*). *Acta Cryst.* A**71**, 3–8.

Sheldrick, G. M. (2015*b*). *Acta Cryst.* C**71**, 3–8.

Sieskind, M., Amann, M. & Ponpon, J. P. (1998). *Appl. Phys. A*, **66**, 655–658.

Stoe & Cie (2019). *X-AREA*. Stoe & Cie, Darmstadt, Germany.

Westrip, S. P. (2010). *J. Appl. Cryst.* **43**, 920–925.

Woińska, M., Chodkiewicz, M. L. & Woźniak, K. (2021). *Chem. Commun.* **57**, 3652–3655.

Acta Cryst. (2021). E**77**, 681–685 Chocolatl Torres *et al.* • $K[HgI_3]\cdot H_2O$ 685

supporting information

Acta Cryst. (2021). E**77**, 681-685   [https://doi.org/10.1107/S2056989021005582]

Refinement of K[HgI$_3$]·H$_2$O using non-spherical atomic form factors

Misael Chocolatl Torres, Sylvain Bernès and Ulises Salazar Kuri

Computing details

Data collection: *X-AREA* (Stoe & Cie, 2019); cell refinement: *X-AREA* (Stoe & Cie, 2019); data reduction: *X-AREA* (Stoe & Cie, 2019); program(s) used to solve structure: *SHELXT2018/2* (Sheldrick, 2015a); program(s) used to refine structure: *olex2.refine 1.3* (Bourhis *et al.*, 2015); molecular graphics: *Mercury* (Macrae *et al.*, 2020) and *OLEX2* (Dolomanov *et al.*, 2009); software used to prepare material for publication: *publCIF* (Westrip, 2010).

Potassium triiodidomercurate(II) monohydrate

Crystal data

K[HgI$_3$]·H$_2$O
M_r = 638.41
Orthorhombic, $Pna2_1$
a = 8.5810 (2) Å
b = 9.2648 (3) Å
c = 11.4073 (4) Å
V = 906.89 (5) Å^3
Z = 4
F(000) = 1072
D_x = 4.676 Mg m^{-3}
Ag $K\alpha$ radiation, λ = 0.56083 Å
Cell parameters from 25947 reflections
θ = 2.2–30.8°
μ = 14.87 mm^{-1}
T = 153 K
Block, colourless
0.06 × 0.05 × 0.03 mm

Data collection

Stoe Stadivari diffractometer
Radiation source: Sealed X-ray tube, Axo Astix-f Microfocus source
Graded multilayer mirror monochromator
Detector resolution: 5.81 pixels mm^{-1}
ω scans
Absorption correction: multi-scan (X-AREA; Stoe & Cie, 2019)
$T_{\min}$ = 0.064, $T_{\max}$ = 0.132
29699 measured reflections
2720 independent reflections
2179 reflections with $I > 2\sigma(I)$
$R_{\rm int}$ = 0.070
$\theta_{\max}$ = 23.6°, $\theta_{\min}$ = 2.2°
$h = -12 \rightarrow 12$
$k = -13 \rightarrow 13$
$l = -16 \rightarrow 16$

Refinement

Refinement on F^2
Least-squares matrix: full
$R[F^2 > 2\sigma(F^2)]$ = 0.021
$wR(F^2)$ = 0.038
S = 0.87
2720 reflections
74 parameters
21 restraints
0 constraints
Primary atom site location: dual
Secondary atom site location: difference Fourier map
Hydrogen site location: difference Fourier map
All H-atom parameters refined
$w = 1/[\sigma^2(F_o^2) + (0.0157P)^2]$ where $P = (F_o^2 + 2F_c^2)/3$
$(\Delta/\sigma)_{\max}$ = 0.0003
$\Delta\rho_{\max}$ = 1.17 e Å^{-3}
$\Delta\rho_{\min}$ = −1.25 e Å^{-3}

Extinction correction: SHELXL2018/3 (Sheldrick 2015b), $Fc^{*}=kFc[1+0.001xFc^{2}\lambda^{3}/\sin(2\theta)]^{-1/4}$

Extinction coefficient: 0.00015 (5)
Absolute structure: Flack (1983)
Absolute structure parameter: 0.033 (11)

Special details

Refinement. Refinement using NoSpherA2, an implementation of NOn-SPHERical Atom-form-factors in Olex2. Please cite: F. Kleemiss *et al.* DOI 10.1039/D0SC05526C - 2020 NoSpherA2 implementation of HAR makes use of tailor-made aspherical atomic form factors calculated on-the-fly from a Hirshfeld-partitioned electron density (ED) - not from spherical-atom form factors.
The ED is calculated from a gaussian basis set single determinant SCF wavefunction - either Hartree-Fock or DFT using selected funtionals - for a fragment of the crystal. This fragment can be embedded in an electrostatic crystal field by employing cluster charges. The following options were used: SOFTWARE: ORCA PARTITIONING: NoSpherA2 INT ACCURACY: High METHOD: PBE BASIS SET: x2c-TZVPP CHARGE: 0 MULTIPLICITY: 1 RELATIVISTIC: DKH2 DATE: 2021-04-12_22-39-08

Fractional atomic coordinates and isotropic or equivalent isotropic displacement parameters (Å²)

	x	*y*	*z*	U_{iso}*/U_{eq}
Hg1	0.25561 (3)	0.70101 (2)	0.500694 (18)	0.02464 (6)
I1	0.25904 (7)	0.42035 (5)	0.56854 (3)	0.02692 (9)
I2	0.49597 (5)	0.77133 (3)	0.33996 (3)	0.01831 (7)
I3	0.23628 (7)	0.92253 (5)	0.65827 (3)	0.02791 (10)
K1	0.44530 (17)	0.15898 (17)	0.3610 (2)	0.0413 (4)
O1	0.6331 (5)	0.4017 (5)	0.3698 (5)	0.0321 (11)
H1a	0.634 (12)	0.437 (11)	0.459 (6)	0.034 (16)
H1b	0.607 (14)	0.498 (9)	0.316 (9)	0.06 (2)

Atomic displacement parameters (Å²)

	U^{11}	U^{22}	U^{33}	U^{12}	U^{13}	U^{23}
Hg1	0.02658 (10)	0.02249 (10)	0.02484 (11)	−0.00072 (11)	0.00067 (13)	−0.00180 (11)
I1	0.0331 (2)	0.0247 (2)	0.02295 (19)	−0.0019 (2)	−0.0010 (2)	0.00594 (16)
I2	0.01527 (15)	0.02130 (15)	0.01837 (17)	0.00014 (15)	−0.00029 (16)	0.0012 (2)
I3	0.0337 (2)	0.0264 (2)	0.0236 (2)	0.0034 (2)	−0.0026 (3)	−0.00697 (17)
K1	0.0251 (7)	0.0278 (7)	0.0711 (13)	0.0039 (5)	−0.0017 (8)	0.0034 (9)
O1	0.030 (2)	0.020 (2)	0.047 (3)	0.0026 (18)	0.002 (2)	−0.002 (2)
H1a	0.02 (4)	0.04 (2)	0.047 (10)	0.007 (15)	0.002 (7)	−0.005 (5)
H1b	0.10 (5)	0.021 (16)	0.05 (2)	0.001 (11)	−0.017 (16)	−0.003 (8)

Geometric parameters (Å, º)

Hg1—I1	2.7131 (5)	I3—K1^{iv}	3.659 (2)
Hg1—I2	2.8356 (5)	I3—K1^{v}	3.7067 (19)
Hg1—I2^{i}	2.8968 (5)	K1—O1^{ii}	2.739 (5)
Hg1—I3	2.7333 (5)	K1—O1	2.769 (5)
I1—K1^{ii}	3.6595 (19)	O1—H1a	1.07 (6)
I1—K1	3.745 (2)	O1—H1b	1.11 (7)
I2—K1^{iii}	3.6257 (16)		
I3—Hg1—I1	122.189 (16)	I2^{vii}—K1—I1	137.19 (6)

I2—Hg1—I1	113.375 (16)	I1^{viii}—K1—I1	92.00 (5)
I3—Hg1—I2	107.267 (15)	I3^{ix}—K1—I1	148.42 (5)
I2^{i}—Hg1—I1	105.885 (15)	I3^{x}—K1—I1	77.82 (3)
I3—Hg1—I2^{i}	107.648 (15)	O1^{ii}—K1—I2^{vii}	85.19 (10)
I2—Hg1—I2^{i}	97.460 (14)	O1—K1—I2^{vii}	137.50 (10)
K1^{ii}—I1—Hg1	90.00 (3)	O1^{ii}—K1—I1^{viii}	130.89 (15)
K1—I1—Hg1	116.37 (3)	O1—K1—I1^{viii}	73.23 (12)
K1^{iii}—I2—Hg1	95.60 (3)	O1^{ii}—K1—I3^{ix}	135.32 (15)
K1^{iii}—I2—Hg1^{vi}	87.86 (3)	O1—K1—I3^{ix}	75.86 (11)
K1^{iv}—I3—Hg1	102.44 (3)	O1^{ii}—K1—I3^{x}	75.34 (12)
K1^{v}—I3—Hg1	86.63 (3)	O1—K1—I3^{x}	74.46 (12)
K1—I1—K1^{ii}	77.01 (4)	O1^{ii}—K1—I1	72.08 (12)
K1^{iv}—I3—K1^{v}	77.50 (4)	O1—K1—I1	72.56 (11)
Hg1—I2—Hg1^{vi}	99.816 (14)	K1—O1—K1^{viii}	113.65 (15)
I2^{vii}—K1—I1^{viii}	75.86 (3)	O1^{ii}—K1—O1	137.29 (12)
I3^{ix}—K1—I2^{vii}	70.37 (3)	H1a—O1—K1^{viii}	95 (5)
I3^{ix}—K1—I1^{viii}	79.52 (3)	H1a—O1—K1	106 (6)
I3^{x}—K1—I2^{vii}	131.42 (6)	H1b—O1—K1^{viii}	110 (6)
I3^{x}—K1—I1^{viii}	147.69 (5)	H1b—O1—K1	121 (6)
I3^{ix}—K1—I3^{x}	93.18 (5)	H1b—O1—H1a	107 (8)

Symmetry codes: (i) *x*−1/2, −*y*+3/2, *z*; (ii) *x*−1/2, −*y*+1/2, *z*; (iii) *x*, *y*+1, *z*; (iv) −*x*+1, −*y*+1, *z*+1/2; (v) −*x*+1/2, *y*+1/2, *z*+1/2; (vi) *x*+1/2, −*y*+3/2, *z*; (vii) *x*, *y*−1, *z*; (viii) *x*+1/2, −*y*+1/2, *z*; (ix) −*x*+1, −*y*+1, *z*−1/2; (x) −*x*+1/2, *y*−1/2, *z*−1/2.

Hydrogen-bond geometry (Å, º)

D—H···*A*	*D*—H	H···*A*	*D*···*A*	*D*—H···*A*
O1—H1*a*···I3^{vi}	1.07	2.76	3.777 (6)	158
O1—H1*b*···I2	1.11	2.72	3.637 (5)	140

Symmetry code: (vi) *x*+1/2, −*y*+3/2, *z*.